Hierarchical composition of reliable recombinase logic devices.

Sarah Guiziou, Pauline Mayonove, and Jerome Bonnet*

Centre de Biochimie Structurale, INSERM U1054, CNRS UMR5048, Université de Montpellier, 29 rue de Navacelles, 34090 Montpellier, France.

*To whom correspondence should be addressed: jerome.bonnet@inserm.fr

ABSTRACT

We provide a systematic framework for engineering reliable recombinase logic devices by hierarchical composition of well-characterized, optimized recombinase switches. We apply this framework to build a recombinase logic device family supporting up to 4-input Boolean logic. This work will support the predictable engineering of several classes of recombinase devices to reliably control cellular behavior.

MAIN TEXT

The field of synthetic biology aims at programming cellular or organismal behavior to address pressing challenges and answer basic research questions[1]. Synthetic biologists inspired from electronics to build biological logic gates operating in living cells[2–4] and responding to specific signal patterns, generally using gene expression as an output. Gates were engineered using transcriptional regulators[5,6], RNA molecules[7], or site-specific recombinases[8–10]. Recombinase logic is of particular interest because of its compact design, modularity, and associated memory. Recombinase logic gates operates by specifically inverting or excising DNA sequences containing regulatory elements flanked by recombination sites. However, different arrangements of multiple recombination sites and regulatory elements can produce devices having variable behavior[11,12]. This problem increases with the numbers of inputs to be computed, and engineering recombinase logic gates is still a trial-and error process. Scaling-up recombinase logic circuits and extending their applications therefore requires simple and accessible engineering frameworks.

We devised a strategy in which a logic function is decomposed into a limited set of subfunctions each performed by a particular strain within a multicellular consortia [13,14]. Each subfunction is executed by a particular recombinase logic device. For a given number of inputs, a fixed, small number of recombinase devices can be differentially combined to obtain all possible logic functions. Recombinase logic devices are obtained by hierarchically combining two classes of logic elements, ID and NOT, according to a specific set of rules[14] (**Fig. 1**). ID-elements implement the IDENTITY function, in which the output is ON when the input is present. In recombinase operated ID-elements, excision of a terminator triggers gene expression. NOT elements implement the NEGATION function, so that the output is ON when the input is absent and vice-versa. In NOT elements, recombinase-mediated excision of a promoter turns-off gene expression.

In our design, assembling higher-order recombinase devices relies on successful functional composition of several ID and NOT elements each responding to a different enzyme and signal. We aimed at experimentally implement this logic system and started by identifying the best working elements from a library containing ID and NOT elements containing all possible permutation and orientations of integrase *attachment* (*att*) sites (**Fig. 2**). We characterized elements responding to four orthogonal serine integrases, Bxb1, TP901-1, Int5 and Int7[11,15] (**Supplementary Fig.1**). All logic elements were based on the same scaffold composed of a strong promoter (P7)[16], a ribozyme (RiboJ) to obtain an identical

5'UTR in all constructs[17], a bicistronic RBS (BCD) to prevent interactions between the RBS and the coding sequence[16] and a superfolder green fluorescent protein (sfGFP) as a reporter[18]. To speed up the process, we directly synthesized all constructs corresponding to the element before and after recombination occurred.

We measured GFP fluorescence intensity in the different states for all constructs, and observed important variation of element behavior depending on integrase site positions and orientations (**Fig.2** and **Supplementary Fig.2-3**). Two NOT elements responding to TP901-1 integrase had leaky GFP expression (6 times above the negative control) in their supposedly OFF-state (**Fig. 2a**), suggesting directional cryptic promoter activities in TP901-1 *att* sites. ID-elements also had important differences depending on integrase site orientations, especially for non-recombined elements, with up to 100-fold difference in gene expression between Int5 elements (**Fig. 2b**). For TP901-1, we observed that all ID-elements expressed GFP in their OFF states and tracked the problem to inefficient termination activity. We obtained a robust ID-element for TP901-1 by using a different terminator (**Fig. 2b**). For each integrase and function, we selected elements having low leakage in their OFF state and the highest switching fold changes, ranging between 250 to 500.

We then composed these elements to obtain fourteen devices capable of implementing all 4-input logic functions[14] (**Fig. 3a**). We characterised the response of these devices to all possible input combinations. To streamline our characterization process, we decoupled recombination from any particular control signal by co-transforming the logic devices with various constitutive gene expression cassettes containing all possible combinations of the four integrases (**Supplementary Fig 4-5**).

All logic devices behaved as expected with very distinct ON and OFF states, demonstrating the possibility to obtain devices operating reliably from well-characterized logic elements (**Fig. 3a**). Some devices had an expression level of GFP above the background in their OFF states while most devices exhibited slightly lower expression levels in their ON states compared to the positive control (i.e. promoter-rbs-GFP). Nevertheless, for all devices, we obtained a fold change between 30 and 300 fold between OFF and ON state (**Supplementary table 1, Supplementary Fig.6**). Additionally, all logic devices had a common output threshold between OFF and ON states within 8-fold change, an essential parameter for a multicellular system containing multiple recombinase devices operating

together. Because of their standardized architecture, these recombinase logic devices can be easily tuned by changing the transcription input signal (**Supplementary Fig. 7)**.

We then aimed at prototyping multicellular logic systems relying on multiple recombinase devices operating in concert. The fact that the system is considered in ON state if at least one strain is ON leads to two challenges. First, the signal strength of all recombinase devices in the ON state must be sufficiently high to be detectable even if a subfraction of the population is ON. Second, the potential GFP leakage observed in certain OFF states **(Fig. 3a)** must be low enough so that the multicellular system does not produce false positives. Different strains expressing various levels of GFP might also exhibit differences in growth rates resulting in the disappearance of some sub-population over time.

To prototype our system, we co-transformed logic devices with the different constitutive integrase cassettes and then mixed different strains in various states to obtain a multicellular system simulating all possible input combination (**Fig. 3b and Supplementary Fig. 4**). We built a two-strain system for 3-input logic and a three strain system for 4-input logic (see online methods for details). We measured the fluorescence intensity of the multicellular system in each input state and were able to clearly distinguish expected ON and OFF states for all systems (**Fig. 3b, 3c,** and **Supplementary Fig. 8**). We did observe differences in ON state intensies, some directly related to the differences of ON level of the separated devices, others to differences in growth rates between strains having different GFP or integrase expression status (**Supplementary Fig. 9**). Despite those differences, these data unambiguously demonstrate the feasibility of composing strains containing recombinase devices to implement complex Boolean functions at the multicellular level.

Here we have demonstrated that standardized, optimized recombinase logic elements can be hierarchically composed into higher-order recombinase logic devices that reliably behave as predicted. We engineered fourteen recombinase logic devices having a common output threshold and demonstrated that they can be combined to implement complex logic functions within automatically designed multicellular systems. Because recombinase activation is entirely decoupled from logic gate operation, these logic devices can be directly used as-is for many applications. Predictable, hierarchical composition of simple logic elements is compatible with other genetic designs using recombinases[11,14,19–22] and will thus extend the robustness and range of applications of this highly useful class of synthetic circuits.

Acknowledgments

We thank members of the synthetic biology group and of the CBS, P. Lemaire and P. Hersen for fruitful discussions. Support was provided by an ERC Starting Grant "Compucell", the INSERM Atip-Avenir program and the Bettencourt-Schueller Foundation. S.G. was supported by a Ph.D. fellowship from the French Ministry of Research and the French Foundation for Medical Research (FRM). The CBS acknowledges support from the French Infrastructure for Integrated Structural Biology (FRISBI) ANR-10-INSB-05-01. Recombinase logic devices and integrase generators are available from Addgene.

Author contributions

S.G. and J.B designed the project. S.G. and P.M. performed and analyzed the experiments. S.G. and J.B. wrote the manuscript.

Competing financial interests

The authors declare no competing financial interest.

SUPPLEMENTARY MATERIALS

1. **Supplementary figures and tables:**

- **Supplementary Fig. 1**: Characterization and orthogonality of 4 serine integrases used in this study.
- **Supplementary Fig. 2**: Detailed histograms of NOT elements characterization.
- **Supplementary Fig. 3**: Detailed histograms of ID elements characterization.
- **Supplementary Fig. 4**: Design and characterization of 16 constitutive integrase expression cassettes.
- **Supplementary Fig. 5**: Schematics of the workflow used to characterize recombinase devices.
- **Supplementary Fig. 6:** Recombinase logic device characteristics.
- **Supplementary Fig. 7:** Recombinase device tuning through change in transcription input signal.
- **Supplementary Fig. 8:** A 4-input multicellular logic system using a device tuned by changing the transcription input signal.

- **Supplementary Fig. 9:** Measurement of proportions between the different strains of a multicellular system at different timepoints.
- **Supplementary Table 1:** Fold changes for recombinase logic devices.

2. DNA sequences

- DNA sequences for NOT and ID elements, recombinase logic devices, and integrase expression cassettes.

3. Experimental data

- Raw data for all logic elements and recombinase devices characterization.

REFERENCES

1. Endy, D. Foundations for engineering biology. *Nature* **438,** 449–453 (2005).
2. Benenson, Y. Biomolecular computing systems: principles, progress and potential. *Nat. Rev. Genet.* (2012).
3. Macia, J. & Sole, R. How to make a synthetic multicellular computer. *PLoS One* **9,** e81248 (2014).
4. Brophy, J. A. N. & Voigt, C. A. Principles of genetic circuit design. *Nat. Methods* **11,** 508–520 (2014).
5. Nielsen, A. A. K. *et al.* Genetic circuit design automation. *Science* **352,** aac7341 (2016).
6. Macia, J. *et al.* Implementation of Complex Biological Logic Circuits Using Spatially Distributed Multicellular Consortia. *PLoS Comput. Biol.* **12,** e1004685 (2016).
7. Green, A. A. *et al.* Complex cellular logic computation using ribocomputing devices. *Nature* **548,** 117–121 (2017).
8. Bonnet, J., Yin, P., Ortiz, M. E., Subsoontorn, P. & Endy, D. Amplifying genetic logic gates. *Science* **340,** 599–603 (2013).
9. Siuti, P., Yazbek, J. & Lu, T. K. Synthetic circuits integrating logic and memory in living cells. *Nat. Biotechnol.* **31,** 448–452 (2013).
10. Weinberg, B. H. *et al.* Large-scale design of robust genetic circuits with multiple inputs and outputs for mammalian cells. *Nat. Biotechnol.* **35,** 453–462 (2017).
11. Bonnet, J., Yin, P., Ortiz, M. E., Subsoontorn, P. & Endy, D. Amplifying genetic logic gates. *Science* **340,** 599–603 (2013).
12. Siuti, P., Yazbek, J. & Lu, T. K. Synthetic circuits integrating logic and memory in living cells. *Nat. Biotechnol.* **31,** 448–452 (2013).
13. Regot, S. *et al.* Distributed biological computation with multicellular engineered networks. *Nature* **469,** 207–211 (2010).

14. Guiziou, S., Ulliana, F., Moreau, V., Leclere, M. & Bonnet, J. An Automated Design Framework for Multicellular Recombinase Logic. *ACS Synth. Biol.* **7,** 1406–1412 (2018).
15. Yang, L. *et al.* Permanent genetic memory with >1-byte capacity. *Nat. Methods* **11,** 1261–1266 (2014).
16. Mutalik, V. K. *et al.* Precise and reliable gene expression via standard transcription and translation initiation elements. *Nat. Methods* (2013).
17. Lou, C., Stanton, B., Chen, Y.-J., Munsky, B. & Voigt, C. A. Ribozyme-based insulator parts buffer synthetic circuits from genetic context. *Nat. Biotechnol.* **30,** 1137–1142 (2012).
18. Pédelacq, J.-D., Cabantous, S., Tran, T., Terwilliger, T. C. & Waldo, G. S. Engineering and characterization of a superfolder green fluorescent protein. *Nat. Biotechnol.* **24,** 79–88 (2005).
19. Bonnet, J., Subsoontorn, P. & Endy, D. Rewritable digital data storage in live cells via engineered control of recombination directionality. *Proc. Natl. Acad. Sci. U. S. A.* **109,** 8884–8889 (2012).
20. Hsiao, V., Hori, Y., Rothemund, P. W. & Murray, R. M. A population-based temporal logic gate for timing and recording chemical events. *Mol. Syst. Biol.* **12,** 869 (2016).
21. Lakso, M. *et al.* Targeted oncogene activation by site-specific recombination in transgenic mice. *Proc. Natl. Acad. Sci. U. S. A.* **89,** 6232–6236 (1992).
22. Pichel, J. G., Lakso, M. & Westphal, H. Timing of SV40 oncogene activation by site-specific recombination determines subsequent tumor progression during murine lens development. *Oncogene* **8,** 3333–3342 (1993).
23. Lutz, R. & Bujard, H. Independent and tight regulation of transcriptional units in Escherichia coli via the LacR/O, the TetR/O and AraC/I1-I2 regulatory elements. *Nucleic Acids Res.* **25,** 1203–1210 (1997).
24. Gibson, D. G. *et al.* Enzymatic assembly of DNA molecules up to several hundred

kilobases. *Nat. Methods* **6,** 343–345 (2009).

25. Guiziou, S. *et al.* A part toolbox to tune genetic expression in Bacillus subtilis. *Nucleic Acids Res.* **44,** 7495–7508 (2016).

Figure 1

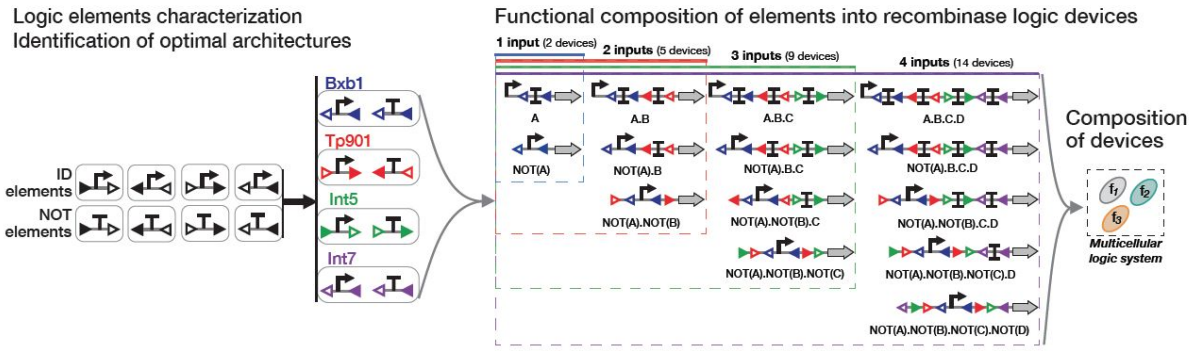

Figure 1: A hierarchical framework for recombinase logic device engineering.

Logic devices are composed from NOT and IDENTITY (ID) elements, respectively composed by being nested or placed in series[14]. First, ID and NOT-elements with all possible integrase-site orientations and permutations are characterized (black triangle: attB site, white triangle: attP site). Elements with the best behavior are selected and composed to design the 14 logic devices required to compute all 4-input Boolean functions. For recombinase logic devices, blue sites (Bxb1 sites) correspond to input A, red sites (TP901-1) to input B, green sites (Int5) to input C and purple sites (Int7) to input D.

Figure 2

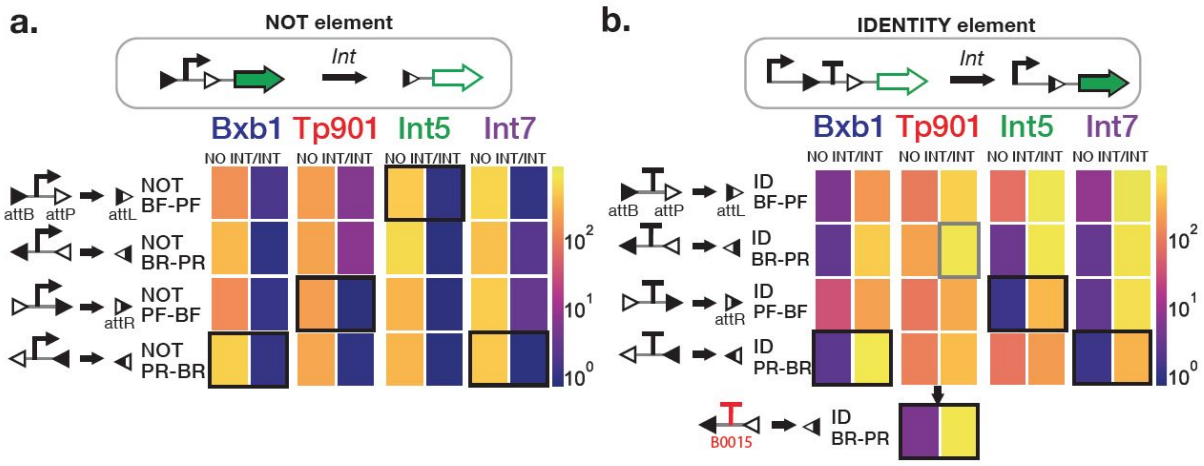

Figure 2: Identification of best working logic elements form a library of NOT and IDENTITY elements.

a. NOT elements are composed of a promoter surrounded by integrase sites. In presence of the integrase, the promoter is excised and expression of the output gene is switched from ON to OFF. **b. IDENTITY elements** are composed of a terminator surrounded by integrase sites. In presence of the integrase, the terminator is excised,and gene expression is switched ON. NOT and IDENTITY elements responding to four integrases (Bxb1, TP901-1, Int5, Int7) were characterized. For each element, four different designs are possible (BF-PF, BR-PR, PF-BP, PR-BR). We measured gene expression before (NO INT) and after switching (INT) by flow cytometry using sfGFP as output. Cells were grown in LB with appropriate antibiotics for 16 hours at 37°C. The data shown in the heatmaps correspond to the fold change in GFP median fluorescence intensity over the negative control (cells with no plasmid). Boxes indicate the construct that was ultimately chosen. A functional TP901-1 ID-element was obtained by replacing the original terminator (lower insert). Data are the mean of 3 experiments performed in 3 different days with 3 replicates per experiment.

Figure 3

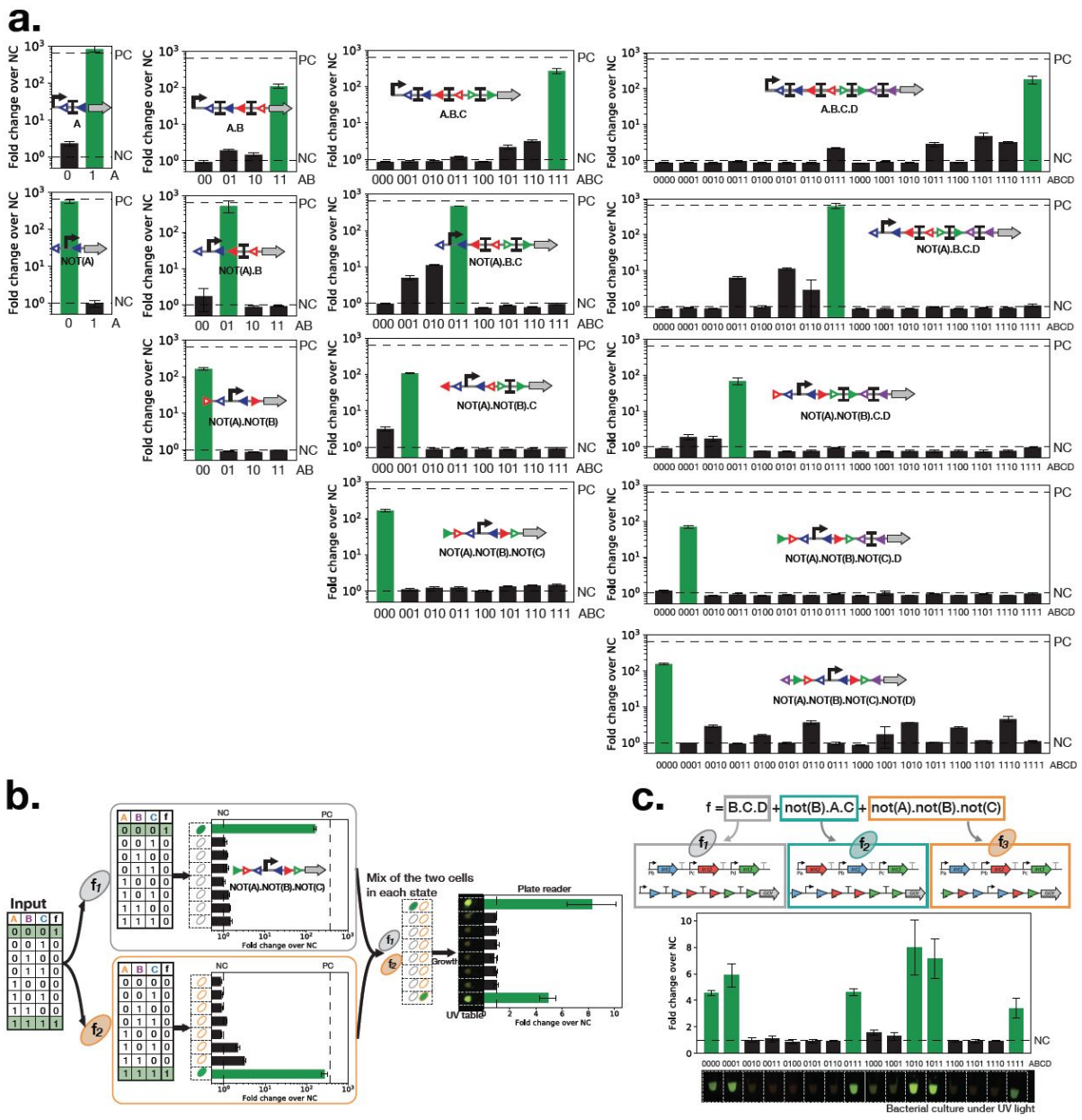

Figure 3: Reliable functional composition of logic elements into recombinase logic devices that support complex multicellular logic.

a. 14 reliable recombinase logic devices composed from standard logic elements. We characterized recombinase logic device for each input state by co-transforming each devices with a combinatorial collection of constitutive integrase cassette (**Supplementary Fig. 4 & 5**). We measured the fluorescence intensity for each state by flow-cytometry. For each device, the bar graph corresponds to the fold change of median GFP fluorescence intensity over the negative control. Corresponding input states are on the x-axis (0: no input, 1: input). Green bars correspond to the input states expected to be ON. Fold changes

for the negative control (NC, no promoter, Fold Change =1) and positive control (PC, promoter only, Fold Change=650) are represented by dash lines (NC and PC). Data are the mean of 3 experiments performed in 3 different days with 3 replicates per experiment. Error bar: +/- SD. **b. Workflow for multicellular logic system prototyping.** The consensus 3-input function is decomposed in two sub-functions implemented using two logic devices. To prototype this logic system for each input state, we mixed the two strains containing the recombinase logic device and different constitutive integrase cassettes corresponding to the different input states. After overnight growth, we measured the bulk fluorescence intensity of the whole-population using a plate reader. Bar graphs corresponds to the fold change in GFP median fluorescence intensity over the negative control. Data are from two experiments performed in different days with three replicates per experiment. Error bars: +/-SD. The photograph correspond to three co-culture replicates for each state centrifuged together, resuspended in 20 µL and observed under a UV light. **c. Prototyping a 4-input, 3-strain multicellular logic system.** The bar graphs and pictures were obtained as in b.

MATERIALS AND METHODS

E. coli strains and media

DH5alphaZ1 [23] *E. coli* strain was used in this study (laciq, PN25-tetR, SpR, deoR, supE44, Delta(lacZYA-argFV169), Phi80 lacZDeltaM15, hsdR17(rK- mK+), recA1, endA1, gyrA96, thi-1, relA1). *E. coli* was grown on LB media with antibiotic corresponding to the transformed plasmid(s). Antibiotics were purchased from Sigma and used at the following concentration: chloramphenicol: 20µg.mL^{-1}, kanamycin: 25µg.mL^{-1}, carbenicillin: 50µg.mL^{-1} (for ampicillin resistance). For co-transformation of two plasmids, the two corresponding antibiotics were used at the previously defined concentration divided by two.

Molecular biology

We used vectors pSB4K5 and J66100 (from parts.igem.org). The pSB4K5 plasmid containing a kanamycin resistance cassette and a pSC101 low-copy origin of replication was used for cloning of BP and LR targets, parts, logic elements and recombinase logic devices. The J66100 plasmid is a derivative of J64100 in which the chloramphenicol resistance cassette was replaced by an ampicillin resistance one. J66100 has a regulated ColE1 origin of replication and was used the cloning integrase cassettes.

All plasmids used in this study were derived from these two vectors and fragments were assembled using one-step isothermal assembly following standard molecular biology procedures[24]. Enzymes for the one-step isothermal assembly were purchased from New England BioLabs (NEB, Ipswich, MA, USA). PCR were performed using Q5 PCR master mix and One-Taq quick load master mix for colony PCR (NEB), primers were purchased from IDT (Louvain, Belgium) and DNA fragment from Twist Bioscience. Plasmid extraction and DNA purification were performed using kits from Biosentec (Toulouse, France). Sequencing was realized by GATC Biotech (Cologne, Germany).

Construction of BP and LR targets.

For Tp901 and Bxb1 targets, the BP and LR targets from Bonnet et al. were used. For Int3, Int4, Int5 and Int7 targets, a template sequence composed of mKate in forward orientation and GFP in reverse orientation was synthesized and assembled in pSB4K5 between sp0 and spN into the pSB4K5 vector. Then, target fragments containing the sequence between the mKate and GFP coding sequences were synthesized and assembled in the previously constructed template sequence.

Construction of parts, elements and devices.

We use as a backbone for logic elements and devices the expression operating unit from Guiziou et al.[25] which contains several spacers optimized for Gibson assembly. The construct was inserted in pSB4K5 (see DNA sequence supplementary file for insertion locus). For the construction of NOT-, IDENTITY-elements, positive and negative controls, the previous construct was used as a template and amplified between sp0 spacerand the beginning of the GFP for one-step isothermal assembly with linear fragments corresponding to each element. For logic devices, the terminator in 3' of the construct was switched from B0015 to L3S3P00.

Construction of integrase cassettes.

A cassette with each Integrase under the control of lac promoter was synthetized and cloned in J66100 plasmid. These cassettes were used to characterize integrase function and orthogonality (Supplementary Fig. 1). To build a combinatorial library of constitutively expressed integrases (Supplementary Fig. 4), we first synthesized a landing pad composed of promoters, terminators, and spacers and cloned it in J66100 (see DNA sequence file for insertion locus). Each integrase was then amplified from the previous Plac construct and inserted separately in the landing pad generated single integrase cassette. All integrase cassettes variants were then built through gibson assembly by combination of these single integrase cassettes.

Flow-cytometer measurements.

Quantification of expression levels in all strains was performed using an Attune NxT flow-cytometer (Thermofisher) equipped with an autosampler. Experiments were performed on 96 wells plates with 3 replicates per plates. For flow cytometry measurements, 20 000 bacteria events were analysed. A gate was previously designed based on forward and side scatter graphs to remove debris from the analysis. GFP fluorescence intensity was measured using excitation by a 488nm laser and a 510/10 nm filter (BL1). RFP excitation was performed by a 561nm laser and filter 615/25 nm (YL2). Voltages used were FFS: 440, SSC: 340, BL1: 360, for all experiments except with BP and LR targets, and BL1: 400 and YL2: 400, for experiments with BP and LR targets. Data were analyzed and presented using the Flow-Jo (Tristar) software.

Characterization of elements.

A glycerol stock from each construct was streaked on LB agar plate supplemented with kanamycin. 96 deep well plates filled with 500µL of LB with kanamycin antibiotic were inoculated with 3 clones from the freshly streaked plates. For all experiments, 3 clones of the negative control strain corresponding to RBS-GFP without promoter and the positive control strain corresponding to P7-RBS-GFP were inoculated. Plates were grown 16 hours at 37°C. Cultures were diluted 40 times on Focusing Fluid and measured on flow-cytometer.

Three experiments with three replicates per experiments were performed for elements, integrase sites and terminators characterizations. Data were analyzed using Flow-Jo. Bacteria events were gated to remove debris from the analysis by plotting FSC-H over SSC-H. For each independent experiment, the median GFP fluorescence intensity of the bacterial population for each replicate was extracted, corresponding to BL1-H median and the fold change over the NC control was calculated. In figures, the mean of fold change between the three experiments is represented, and the error bar corresponds to the standard deviation between the three experiments.

Characterization of integrases cassettes.

For integrase characterization, each Plac-integrase plasmids and dual controller for Tp901 integrase[11] was co-transformed with BP targets. For constitutive integrase cassette characterization, each constitutive integrase cassette was co-transformed with the BP targets corresponding to the integrase that it should express.

For both experiments, 96 deep wells plate filled with 500µL of LB per well were inoculated with 3 clones per co-transformation and 3 clones per control corresponding to the BP target and LR target strains. For integrase characterization with Plac-integrase plasmid and dual controller plasmid, LB was supplemented with 100µM of IPTG for co-transformation with Plac-integrase and 1% of Arabinose for co-transformation with the dual controller for expression of Tp901. Plates were grown 16 hours at 37°C. Cultures were diluted 40 times on Focusing Fluid and directly measured on flow-cytometer according to previously described methods.

Data analysis was performed using Flow-Jo. Bacteria events were gated to remove debris from the analysis by plotting FSC-H over SSC-H. Data were represented using a density plot of BL1-H over YL2-H, corresponding to the GFP fluorescence intensity over the RFP fluorescence intensity. The proportions of bacteria in BP or LR states were obtained using BL1-H over YL2-H plot by gating the population corresponding to the BP or LR target strain. Data represented in the heatmap correspond to the mean of the proportion obtained for the three replicates in one experiment.

Characterization of recombinase logic devices.

Each device was co-transformed with each integrase cassettes corresponding to its input number. For each transformation, 3 clones were picked and inoculated in 500mL of LB in 96 deep well plate. Additionally, the negative control (RBS-GFP without promoter) strain and positive control (Promoter-RBS-GFP) strain were streaked from glycerol stocks and 3 clones were picked and inoculated. Plates were grown 16 hours at 37°C. Cultures were diluted 40 times on Focusing Fluid and measured on flow-cytometer. Two experiments with three replicates per experiments were performed. Data were analyzed using Flow-Jo using the same procedure than the one detailed previously for element characterizations.

Multicellular logic system prototyping.

Devices were co-transformed with corresponding constitutive integrase cassettes. Three clones per transformation were inoculated in 500µL of LB in 96 deep well plate. Plates were incubated during 16 hours at 37°C to reach stationary phase. From the stationary phase culture, cells were mixed in identical proportions and diluted 1000 times for growth in 500µL of LB in 96 deep well plate. Plates were incubated 16 hours at 37°C. The co-cultures were diluted 4 times in PBS and analyzed using a plate reader for measurement of bulk fluorescence intensity. Additionally, co-cultures were diluted 200 times in focusing fluid and analyzed on flow-cytometer. Finally, the three replicates were mixed, centrifuged, ant the cell pellets were resuspended in 20µL of PBS in PCR tubes and imaged under UV tables. Plate reader measurement were performed using a BioTek Cytation 3. GFP fluorescence intensity (Excitation: 485nm, Emission: 528 nm and 85 gain) and absorbance at 600nm were measured. For each sample, GFP fluorescence intensity over absorbance at 600nm were calculated and the mean value was calculated between the three replicates. The fold change over the negative control was determined from this mean value over the one of the Negative control. The error bars correspond to standard deviation in fold change. Flow-cytometry experiments were performed as detailed in the corresponding section. To determine the proportion of cells in ON state (expressing GFP), a first gate was performed

to select bacteria events using FSC-H over SSC-H density plot. A second gate was performed from bacteria events to select single cells using SSC-A over SSC-H density plot. Finally, from single cell event, BL1-H histogram was plotted and cells with more than 4200 fluorescence intensity in arbitrary units were considered ON to determine the proportion of ON cells using a final gate. This procedure was used to analyse flow-cytometry experiments before and after co-culture growth.